Supporting Information Text

Results

Functional Connectivity Between Hippocampal Subfields. We aimed to begin testing the possibility that the convergence of both the trisynaptic pathway (TSP) and monosynaptic pathway (MSP) on area CA1 (Figure S4B) may result in competition between episodic memory and statistical learning (Schapiro et al., 2017). We analyzed the fMRI data from Experiment 3 using a task-based functional connectivity approach known as psychophysiological interaction (PPI). We reasoned that statistical learning would be reflected in MSP connectivity (e.g., lesioning MSP but not TSP in a model of the hippocampus eliminates statistical learning; (Schapiro et al., 2017)), and thus that EC-CA1 connectivity during encoding would be negatively related to subsequent episodic memory.

We compared hippocampal subfield interactions during time periods when A and B categories were presented ("Structured") to periods when X categories were presented ("Random"). The Structured periods provided an opportunity for both episodic encoding and the extraction of regularities, whereas the Random periods permitted only episodic encoding. Thus, by contrasting Structured vs. Random periods we attempted to isolate the impact of statistical learning on functional connectivity. We did not separate A and B categories in this analysis because the model on which we based this approach (Schapiro et al., 2017) showed MSP engagement by both members of a pair.

We first compared overall CA1 connectivity with EC (reflecting MSP engagement) vs. CA2/3/DG (reflecting TSP engagement) during the Structured periods, but did not find a reliable difference ($t(35) = -0.88$, $p = 0.39$). Likewise, CA1 connectivity did not differ between CA2/3/DG vs. EC during the Random periods ($t(35) = -0.22$, $p = 0.83$). There were also no overall differences within pathway across conditions: CA1 connectivity with EC (MSP) was not reliably greater for the Structured condition ($t(35) = -0.36$, $p = 0.72$), and CA1 connectivity with CA2/3/DG (TSP) was not reliably greater for the Random

condition ($t(35) = 0.82$, $p = 0.42$).

Although it was possible that the Structured condition would have consistently engaged the MSP across participants in the analyses above, our specific hypothesis was that MSP connectivity would be negatively related to episodic encoding. We took advantage of variability in the impact of statistical learning on episodic memory across participants to examine this relationship. For this analysis we quantified episodic memory using A' instead of hit rate, as in the main results, as our goal was a more global measure of memory fidelity rather than to examine condition differences and trial-level interference.

We separately correlated EC $\leftrightarrow$ CA1 (MSP) and CA2/3/DG $\leftrightarrow$ CA1 (TSP) connectivity from the PPI analysis during the Structured periods with A' for Structured A and B items, and likewise the MSP and TSP connectivity during the Random periods with A' for Random X items (Figure S4C). Consistent with our hypothesis, MSP connectivity during Structured periods was negatively related to episodic memory performance ($r = -0.41$, bootstrap $p = 0.0086$, two-tailed), whereas TSP connectivity had no relationship ($r = 0.062$, bootstrap $p = 0.67$, two-tailed); these two correlations significantly differed (bootstrap $p = 0.037$, two-tailed). Neither MSP ($r = -0.039$, bootstrap $p = 0.82$, two-tailed) nor TSP ($r = 0.15$, bootstrap $p = 0.41$, two-tailed) connectivity during Random periods was related to episodic memory performance. Thus, greater MSP engagement in response to regularities reflects a bias away from episodic memory.

Methods

PPI Analysis. We conducted a PPI analysis to explore how statistical learning affected functional connectivity between hippocampal subfields and in turn how this impacted episodic memory. We limited this analysis to the second and third runs of the encoding phase for greater confidence that the regularities had been learned. We concatenated the aligned, normalized residual timecourses from the pre-processing GLM across these two runs. We averaged the activity of voxels in each ROI to compute a mean timecourse for CA1, CA2/3/DG, and EC. Ad-

ditionally, we extracted the onsets of Structured (A & B) and Random (X) pictures, and convolved these two condition regressors with a double-gamma hemodynamic response function (fmrisim function in BrainIAK, http://brainiak.org). We then ran a GLM in R (https://cran.r-project.org/), predicting the CA1 timecourse from a linear combination of regressors for the timecourses of CA2/3/DG and EC, task events in the two conditions (Structured and Random), and the interaction between ROIs and conditions. The interaction regressors were defined as the products of the ROI and condition timecourses (EC*Structured, EC*Random, CA2/3/DG*Structured, CA2/3/DG*Random). Each regressor, as well as the CA1 timecourse, was z-scored and entered simultaneously into the model. A separate model was run for each participant, resulting in one coefficient per regressor per participant. For an interaction regressor of interest, the coefficients were correlated across participants with A' in the memory test for the corresponding condition.

Searchlight Analysis. We conducted a searchlight analysis to explore the specificity of our Prediction of B results in the brain. Using the searchlight function in BrainIAK, we repeated the category decoding analysis in 27-voxel cubes centered on all functional voxels. Each aligned, normalized residual volume from the pre-processing GLM was registered to standard space. These volumes were masked for each searchlight cube and the retained voxels were subjected to the same decoding pipeline described in the main text for the ROIs. The result was a searchlight map per participant, in which the value at each voxel reflected the average classification accuracy for the cube centered at that voxel. The reliability of these maps was assessed at the group level using non-parametric randomization tests (randomise function in FSL) (Winkler et al., 2014), corrected for multiple comparisons using threshold-free cluster enhancement (Smith and Nichols, 2009). As a control analysis, we ran the same searchlight procedure for Perception of B.

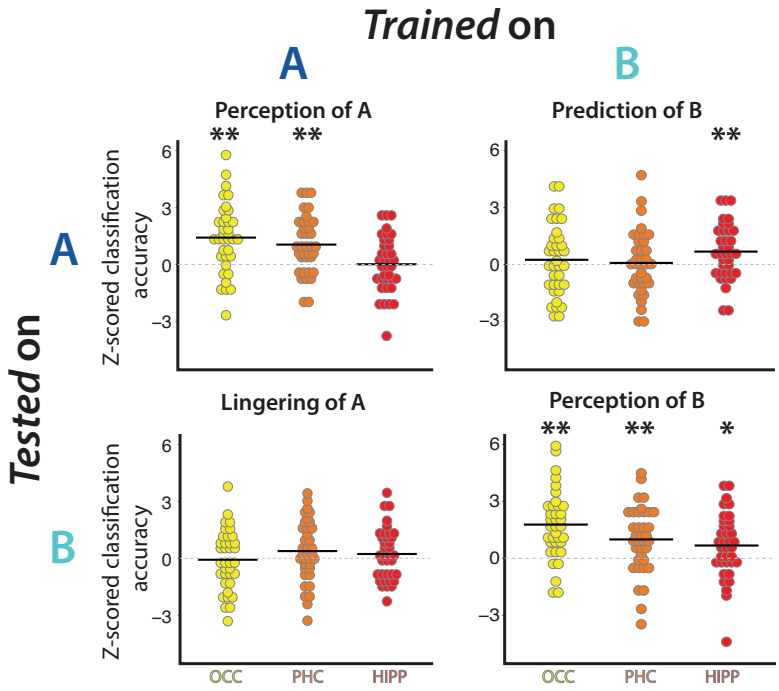

Figure 1: Category Decoding in fMRI Experiment. Z-scored classification in occipital cortex (OCC), parahippocampal cortex (PHC), and hippocampus (HIPP) plotted for each of the four combinations of training or testing on A or B categories. Z-scores were computed by generating a permuted null distribution of classification accuracy values for each participant and calculating the z-score of each participant's empirical classification accuracy relative to their own null distribution. For every A/B combination and ROI, each dot is one participant and the black line is the mean across participants. Perception of A: OCC: $t(35) = 4.65$, $p < 0.001$; PHC: $t(35) = 4.18$, $p < 0.001$; HIPP: $t(35) = 0.043$, $p = 0.97$. Prediction of B: OCC: $t(35) = 0.79$, $p = 0.43$; PHC: $t(35) = 0.29$, $p = 0.77$; HIPP: $t(35) = 2.79$, $p = 0.0084$. Lingering of A: OCC: $t(35) = -0.29$, $p = 0.77$; PHC: $t(35) = 1.43$, $p = 0.16$; HIPP: $t(35) = 1.00$, $p = 0.33$. Perception of B: OCC: $t(35) = 5.89$, $p < 0.001$; PHC: $t(35) = 3.38$, $p = 0.0018$; HIPP: $t(35) = 2.36$, $p = 0.024$. *$p < 0.05$; **$p < 0.01$

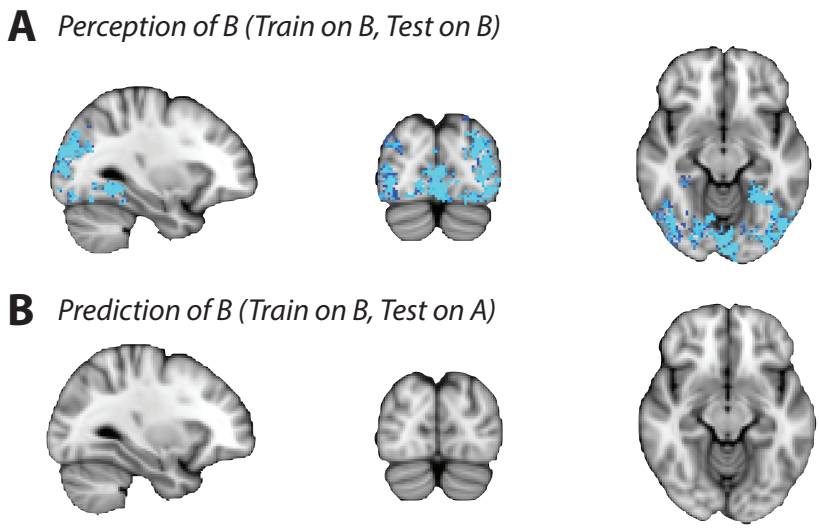

Figure 2: Searchlight results. A) Statistical map for the "Perception of B" searchlight (corrected $p < 0.005$). B) Statistical map for the "Prediction of B" searchlight (corrected $p < 0.005$). Corrections for multiple comparisons performed with TFCE. Statistical maps are plotted on the T1 MNI standard brain (2mm), at slices X = -30 (sagittal), Y = -82 (coronal), Z = -12 (axial).

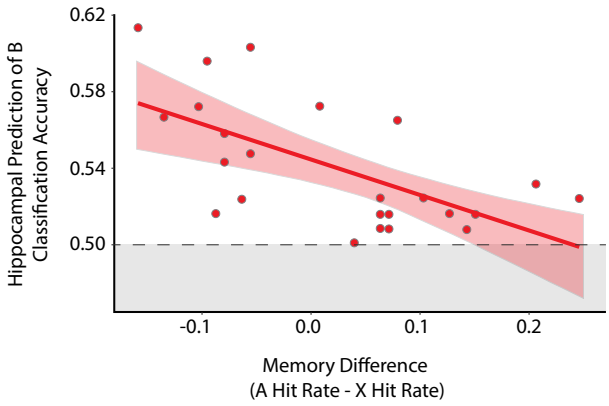

Figure 3: Relation between hippocampal "Prediction of B" classification accuracy and difference in hit rate between A and X, excluding participants with classification accuracy at or below chance (<0.5), marked by gray shading. The negative correlation holds when excluding these participants, showing that they were not driving the overall effect. Error shading indicates bootstrapped 95% confidence intervals.

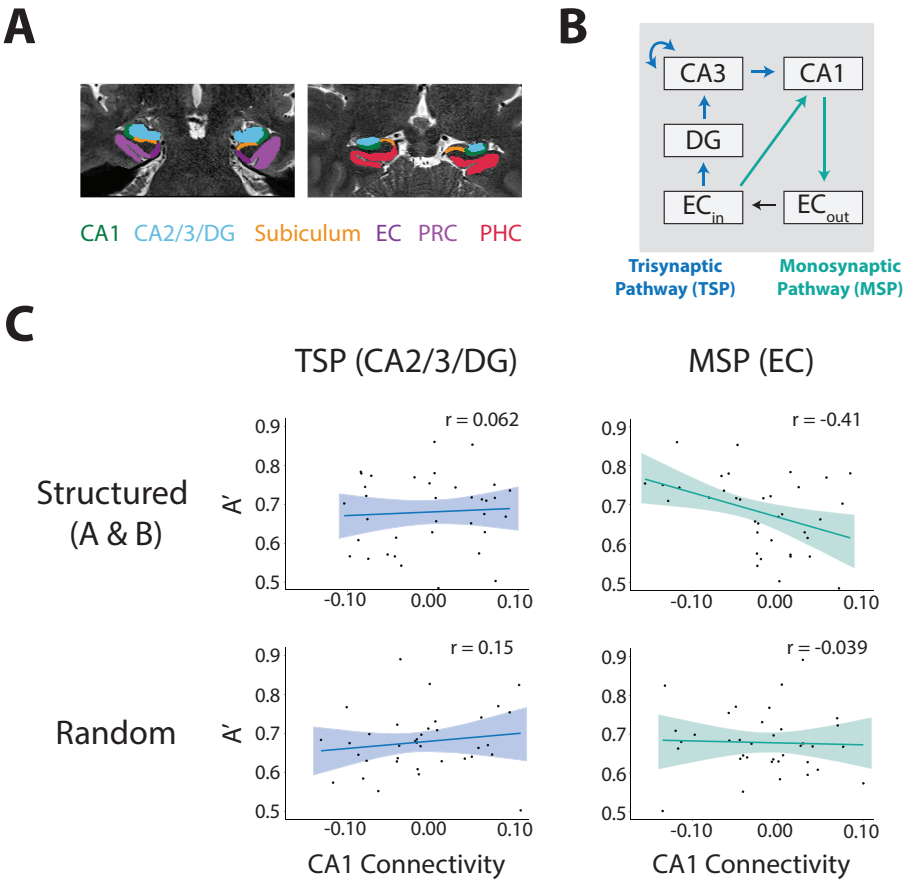

Figure 4: Hippocampal Connectivity in fMRI Experiment. A) Manually segmented hippocampal subfield and MTL cortical ROIs (anterior and posterior slices from representative participant shown): CA1, combined CA2/3/DG, subiculum, entorhinal cortex (EC), perirhinal cortex (PRC), and parahippocampal cortex (PHC). B) Two pathways in the hippocampal circuit: trisynaptic pathway (TSP, blue) and monosynaptic pathway (MSP, teal). C) Relationship of CA1 functional connectivity in TSP (left; CA2/3/DG) and MSP (right; EC) with episodic memory performance (A′) across participants, separated into time periods with (Structured) and without (Random) regularities for statistical learning. Error shading indicates bootstrapped 95% confidence intervals.

References

Schapiro, A.C., Turk-Browne, N.B., Botvinick, M.M., Norman, K.A., 2017. Complementary learning systems within the hippocampus: a neural network modelling approach to reconciling episodic memory with statistical learning. Philosophical Transactions of the Royal Society B: Biological Sciences 372, 20160049.

Smith, S.M., Nichols, T.E., 2009. Threshold-free cluster enhancement: addressing problems of smoothing, threshold dependence and localisation in cluster inference. Neuroimage 44, 83–98.

Winkler, A.M., Ridgway, G.R., Webster, M.A., Smith, S.M., Nichols, T.E., 2014. Permutation inference for the general linear model. Neuroimage 92, 381–397.